AIAA JOURNAL
Vol. 33, No. 3, March 1995

Effect of Concentrated Mass on Stability of Cantilevers Under Rocket Thrust

Yoshihiko Sugiyama* and Jun Matsuike†
University of Osaka Prefecture, Sakai-shi 593, Japan
Bong-Jo Ryu‡
Taejon National University of Technology, Taejon 300-172, Republic of Korea
and
Kazuo Katayama,§ Shigeru Kinoi,¶ and Norio Enomoto**
Dicel Chemical Industries, Ltd., Hyogo-ken 671-16, Japan

The paper describes the effect of an intermediate concentrated mass on the dynamic stability of cantilevered columns subjected to a rocket thrust. It is assumed that the rocket thrust is produced by the installation of a solid rocket motor at the tip end of the cantilevered columns having the intermediate mass. The rocket motor is assumed to be a rigid body having finite sizes but not a mass point. The importance of the magnitude and size of the intermediate mass is demonstrated by theory and experiment. The experimental results are compared with theoretical predictions made by taking into account the mass and size of the rocket motor as well as intermediate mass effect. The internal damping was neglected in the theoretical predictions. It is shown that theoretical stability predictions and experimental flutter limits agreed well.

Nomenclature

a = element of an intermediate mass
b = column width
EI = flexural rigidity of a column
F = follower force
F^* = dimensionless follower force
F^*_{cr} = dimensionless flutter load
h = column thickness
i = ith element of the column
J_1 = rotary inertia of an intermediate mass
J_2 = rotary inertia of a rocket motor
$[K]$ = global stiffness matrix
L = length of a column
L_R = length between tip end of the column and center of gravity of the rocket motor
ℓ = length of a column element
$[M]$ = global mass matrix
m = mass per unit length of a column
N = total number of the element or element of the rocket motor
T = kinetic energy
t = time
V = elastic potential energy
W_c = work done by conservative component of applied load
x = axial coordinate of a column
x' = local coordinate of axial direction
x'_{m1} = local coordinate of an intermediate mass position
x'_{m2} = local coordinate of a rocket motor position
y = deflection of a column
α_1 = dimensionless intermediate mass
α_2 = dimensionless mass of a rocket motor
β_1 = dimensionless rotary inertia of an intermediate mass
β_2 = dimensionless rotary inertia of a rocket motor
δW_N = virtual work done by nonconservative component of applied load
μ_1 = dimensionless position of an intermediate mass
μ_2 = dimensionless position of a rocket motor
ξ = dimensionless local coordinate of axial direction
ξ_{m1} = dimensionless local position of an intermediate mass
ξ_{m2} = dimensionless local position of a rocket motor
σ = dimensionless length between tip end of the column and center of gravity of the rocket motor
Ω = eigenfrequency
$\{\}$ = vector notation

Received March 21, 1994; presented as Paper 94-1622 at the AIAA/ASME/ASCE/AHS/ASC 35th Structures, Structural Dynamics, and Materials Conference, Hilton Head, SC, April 18–20, 1994; revision received Sept. 7, 1994; accepted for publication Nov. 28, 1994.

*Professor, Department of Aerospace Engineering. Member AIAA.
†Graduate Student, Department of Aerospace Engineering.
‡Assistant Professor, Department of Mechanical Design Engineering, 305 Samsung 2-dong, Dong-ku. Member AIAA.
§Manager, Technical Research and Development Center, Harima Plant.
¶General Manager.
**Staff Engineer.

I. Background

DYNAMIC stability of aerospace structures under a follower force has been studied by many researchers.[1,2] A thrust force induced by a jet or a rocket engine is a typical follower force and thus may cause the flutter instability in flexible aerospace structures.

The stability of a cantilevered column under a follower force at the free end was first investigated by Beck.[3] The problem of a column carrying a concentrated tip mass was presented by Pflüger.[4] He assumed the mass as a mass point but not a rigid body. Barsoum[5] used the finite element method (FEM) for the problem of stability of a nonconservative system. He proposed the extended applicability of the finite element method to include nonconservative forces in the stability analysis of linear elements. Kounadis and Katsikadelis[6] discussed the effect of three concentrated masses and their positions on the dynamic stability of columns. Park and Mote[7] investigated the maximum controlled follower force on a free-free beam carrying a concentrated mass. They verified the importance of the preceding mass position and its magnitude and predicted the magnitude of the follower force for stable transverse motion of the free-free beam. Chen and Ku[8] studied the stability of a cantilevered column under distributed follower force by taking into account shear deformation and rotary inertia. After that, they[9] developed eigenvalue sensitivity analysis of Beck's column with a concentrated mass at the free end. They also demonstrated that the critical flutter load is influenced more effectively by transverse shear deformation than by rotary inertia. However, the discussions so far made have been mostly theoretical, and the tip mass has been assumed to be a mass point. Recently, Sugiyama et al.,[10] have worked on the stability of cantilevered columns through both experiment and theory.

The aim of the paper is to give an experimental verification of theoretical prediction on the dynamic stability of a cantilevered column subjected to a follower force. The effects of an intermediate mass and its position are also discussed in the present paper.

II. Finite Element Method Formulation

Figure 1 shows a uniform cantilevered column subjected to a rocket thrust F. The column has a total length L, flexural rigidity EI, and mass per unit length m. The rocket motor is now considered as a rigid body having mass M_2 and rotary inertia J_2. The distance from the tip of the column to the gravity center of the rocket motor is denoted by L_R, and hereafter called the motor distance. An intermediate concentrated mass (hereafter called the intermediate mass) having magnitude M_1 and rotary inertia J_1 is attatched to the column at x_{m1} apart from the fixed end.

Extended Hamilton's principle for the nonconservative system under consideration can be written in the form

$$\int_{t_1}^{t_2} \{\delta(T - V + W_c)\}\,\mathrm{d}t + \int_{t_1}^{t_2} \delta W_N\,\mathrm{d}t = 0 \tag{1}$$

where the functionals are given by

$$\begin{aligned} T = \frac{1}{2}\int_0^L \left(m \cdot y_t^2\right)\mathrm{d}t + \tfrac{1}{2}M_2\big(y_t^2 + 2L_R \cdot y_t \cdot y_{tx} \\ + L_R^2 \cdot y_{tx}^2\big)\Big|_{x=L} + \tfrac{1}{2}M_1 \cdot y_t^2\Big|_{x=x_{m1}} \\ + \tfrac{1}{2}J_1 \cdot y_{tx}^2\Big|_{x=x_{m1}} + \tfrac{1}{2}J_2 \cdot y_{tx}^2\Big|_{X=L} \end{aligned} \tag{2}$$

$$V = \frac{1}{2}\int_0^L EI \cdot y_{xx}^2\,\mathrm{d}x \tag{3}$$

$$W_c = \frac{1}{2}\int_0^L F \cdot y_x^2\,\mathrm{d}x \tag{4}$$

$$\delta W_N = -F \cdot y_x(L, t) \cdot \delta y(L, t) \tag{5}$$

To apply the finite element method to the system, the column structure is divided into N segments having an equal length of ℓ as shown in Fig. 2.

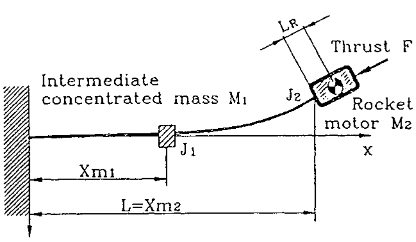

Fig. 1 Mathematical model of a cantilevered column subjected to a rocket thrust at its free end and having an intermediate mass.

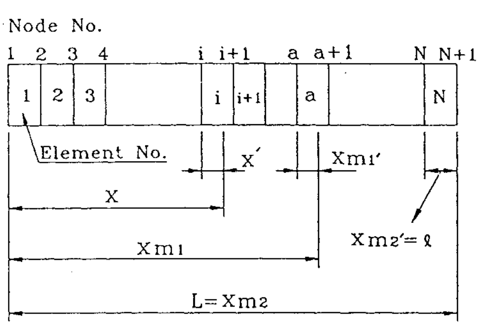

Fig. 2 Finite element model of the column.

It will be convenient to deal with dimensionless forms of the equations. To this end, the following local coordinates and dimensionless quantities are introduced:

$$\begin{aligned} x' = x - (i-1)\ell, \qquad x'_{m1} = x_{m1} - (a-1)\ell \\ x'_{m2} = L - (N-1)\ell \end{aligned} \tag{6}$$

$$\begin{aligned} \xi = x'/\ell, \qquad \xi_{m1} = x'_{m1}/\ell, \\ \xi_{m2} = x'_{m2}/\ell, \qquad \eta = y/\ell \end{aligned} \tag{7}$$

The local coordinates ξ, ξ_{m1}, and ξ_{m2} satisfy the following relations:

$$\mu_1 = x_{m1}/L, \qquad \mu_2 = x_{m2}/L, \qquad \mu = x/L \tag{8}$$

Substituting of Eqs. (2–7) into Eq. (1) and assuming the solution in the form of Eq. (9) give the following discretized equation:

$$\eta(\xi, t) = \eta(\xi)e^{st} \tag{9}$$

$$\begin{aligned} &\sum_{i=1}^{N}\int_0^1 \left[\frac{\Omega^2}{N^4}\eta^{(i)}\delta\eta^{(i)} + \eta_{\xi\xi}^{(i)}\delta\eta_{\xi\xi}^{(i)} - \frac{F^*}{N^2}\eta_\xi^{(i)}\delta\eta_\xi^{(i)}\right]\mathrm{d}\xi \\ &+ \frac{\alpha_1}{N^3}\eta(\xi_{m1})^{(a)}\delta\eta(\xi_{m1})^{(a)} + \frac{\beta_1}{N}\eta_\xi(\xi_{m1})^{(a)}\delta\eta_\xi(\xi_{m1})^{(a)} \\ &+ \frac{\alpha_2}{N^3}\eta(\xi_{m2})^{(N)}\delta\eta(\xi_{m2})^{(N)} + \frac{\beta_2}{N}\eta_\xi(\xi_{m2})^{(N)}\delta\eta_\xi(\xi_{m2})^{(N)} \\ &+ \frac{\alpha_2\Omega^2\sigma}{N^2}\eta_\xi(\xi_{m2})^{(N)}\delta\eta(\xi_{m2})^{(N)} \\ &+ \frac{\alpha_2\Omega^2\sigma^2}{N}\eta_\xi(\xi_{m2})^{(N)}\delta\eta_\xi(\xi_{m2})^{(N)} \\ &+ \frac{\alpha_2\Omega^2\sigma}{N^2}\eta(\xi_{m2})^{(N)}\delta\eta_\xi(\xi_{m2})^{(N)} \\ &+ \frac{F^*}{N^2}\eta_\xi(1)^{(N)}\delta\eta(1)^{(N)} = 0 \end{aligned} \tag{10}$$

where the following dimensionless parameters are introduced:

$$\begin{aligned} \Omega^2 = mL^4s^2/EI, \qquad F^* = FL^2/EI \\ \alpha_1 = M_1/mL, \qquad \alpha_2 = M_2/mL \\ \beta_1 = J_1/mL^3, \qquad \beta_2 = J_2/mL^3, \qquad \sigma = L_R/L \end{aligned} \tag{11}$$

In Eq. (10), the following shape function vector satisfying the compatibility condition is also introduced:

$$a^T(\xi) = \{1-3\xi^2+2\xi^3 \quad \xi-2\xi^2+\xi^3 \quad 3\xi^2-2\xi^3 \quad -\xi^2+\xi^3\} \tag{12}$$

Finally the following characteristic equation can be obtained:

$$\{\Omega^2[M] + [K]\} \quad \{U\} = \{0\} \tag{13}$$

The stability or instability is determined by investigating the eigenfrequency Ω of the Eq. (13). Only flutter-type instability can take place in the considered problem.

In general, eigenvalues Ω_1 and Ω_2 of the Eq. (13) approach each other on the imaginary axis with increasing F until they coincide and then become complex eigenvalues as the follower force is increased beyond the critical follower force F_{cr}. Therefore, if F is greater than F_{cr}, the first eigenvalue Ω_1 is shifted on the right half-plane of the complex plane, which denotes that the system is unstable.

All of the numerical results in this paper have been obtained with the column divided into 20 elements, so that the discretized system has 20 degrees of freedom.

III. Rocket Motor

Figure 3 shows the thrust curve for a rocket motor to be used in the present experiment.

The rocket motor was considered as a rigid body having average constant mass of 4.05 kg. The average thrust of the rocket motor was assumed to be a constant value of 62.1 kgf (609 N) during the burn out time of 3.2 s. The mass of the powders was 0.90 kg.

The details of the rocket motor are listed in Table 1.

Table 1 Details of rocket motor

Average mass M_2, kg	4.05
Average thrust, kgf	62.1
Burn out time, s	3.2
Rotary inertia J_2, kg · m^2	0.0284
Motor distance L_R, m	0.15284

Table 2 Details of intermediate masses

Intermediate mass	*A*	*B*
Magnitude M_1, kg	1.0	2.3
Rotary inertia J_1, kg · m^2	5.74×10^{-4}	2.03×10^{-2}

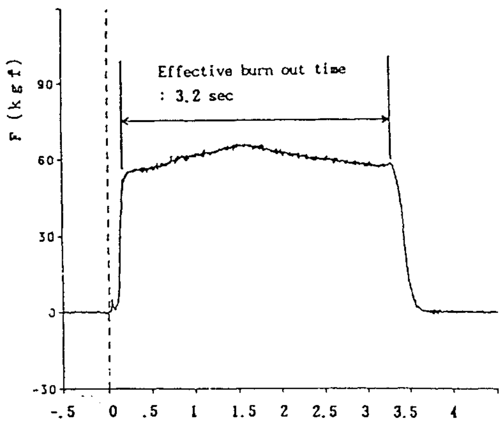

Fig. 3 Thrust curve of the rocket motor.

IV. Effect of an Intermediate Mass

Two different sizes of the intermediate mass were designed for experiment, and they were measured to be 1.0 and 2.3 kg. The details of the intermediate mass are shown in Table 2.

Intermediate masses were made of brass block with hollow rectangular cross section and fixed to the test column by bolts.

The intermediate mass was assumed to be located at position $\mu_1 = 0.6$. The reason why the intermediate mass was attached to the column at $\mu_1 = 0.6$ is explained in Figs. 4a and 4b, which show the effect of the designed intermediate masses on the ratio of critical follower force with an intermediate mass and that without intermediate mass. Especially, the importance of the intermediate mass position is emphasized in these figures.

The designed intermediate masses have mostly a destabilizing effect on the flutter boundary, whereas they are slightly stabilizing only when they are located at the tip end of the column. The intermediate masses were mounted to the column at $\mu_1 = 0.6$ where the highest destabilizing effect takes place.

V. Test Columns

The dimensions of the test columns can be determined on the basis of the theoretical predictions made by FEM analysis. Theoretical predictions of the critical follower forces with the values $M_1 = 0.0$ and $M_2 = 0.0$ were investigated by that of Beck's column in Ref. 2 to investigate the sensitivity of the solution. The result of $F^* = 20.04517$ agreed well with Beck's value of $F^* = 20.05$. The difference is only 0.024%.

The test columns were chosen such that the thrust of the rocket motor from Fig. 3 would reveal the important phenomena pertaining to flutter.

The final dimensions of the test columns were determined to have the cross section of 7.0 × 30 mm and the length of 1100–1200 mm. The details of the test columns are given in Table 3.

VI. Experiment

The schematics of the experimental setup are sketched in Fig. 5. The test column and the rocket motor mounted to the tip end of the column were suspended in space by a thin wire hung from the ceiling. Thus the small motion of the column was restricted to motion in the horizontal plane. Four test runs were conducted in the present experiment.

Photographs of flutter motions observed in the test run number 3 are shown in Figs. 6a and 6b. The photographs were taken at an interval of 0.167 s by the motor-driven camera.

Figure 7 shows the corresponding displacement curve in the test run number 3. The nonlinear effect was not considered in the

Table 3 Details of test columns

Thickness h, mm	7.0
Width b, mm	30.0
Length L, mm	1100–1200
Mass per unit length m, kg/m	0.567
Bending stiffness EI, N · m^2	58.8

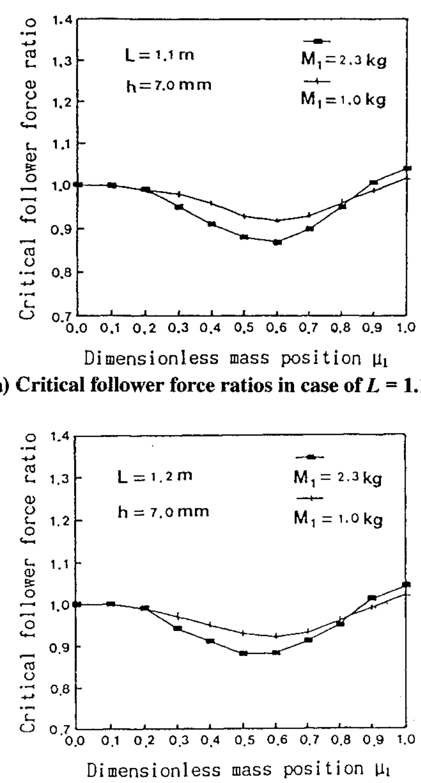

a) Critical follower force ratios in case of L = 1.1 m

b) Critical follower force ratios in case of L = 1.2 m

Fig. 4 Effect of intermediate mass position on the critical follower force.

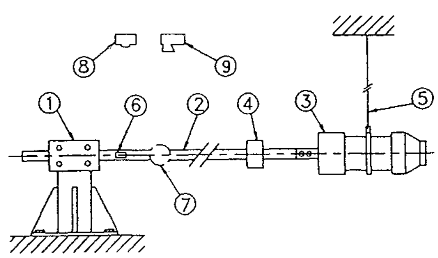

① Clamped end
② Test column
③ Solid rocket motor
④ Intermediate concentrated mass
⑤ Thin wire from the ceilng
⑥ Strain gauges for axial strain measurement
⑦ Target disk for displacement measurement
⑧ Motor-driven Camera
⑨ Video camera

Fig. 5 Schematics of the experimental setup.

Table 4 Test results

Test run no.	Length of column L, mm	Intermediate mass M_1, kg	Position of the intermediate mass x_{m2}, mm	Average thrust F, kgf	Stability
1	1200	0.0	No mass	62.0	Violent flutter
2	1100	0.0	No mass	62.0	Stable
3	1100	2.3	660	62.0	Flutter
4	1100	1.0	660	62.0	Quasistable

a) Flutter motion at 2.00 s

b) Flutter motion at 2.167 s

Fig. 6 Observed flutter motions in test run 3.

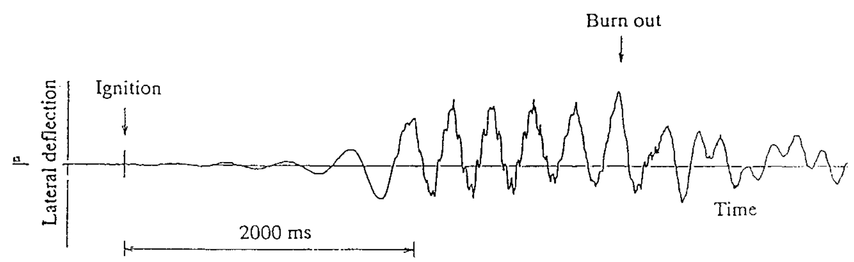

Fig. 7 Dynamic response in the test run 3.

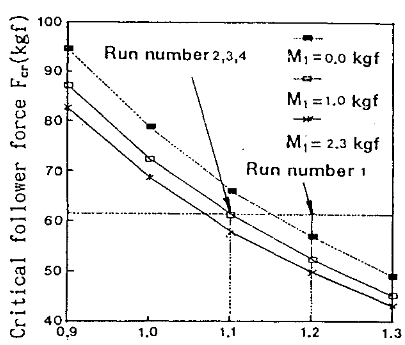

Fig. 8 Theoretical predictions of the critical follower thrust and the test run numbers (μ_1 = 0.6).

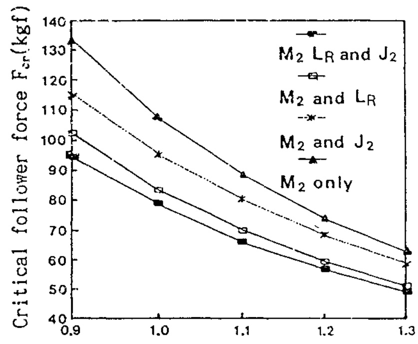

Fig. 9 Effect of three parameters M_2, J_2, and L_R on the critical follower force without an intermediate mass.

analysis. Of course, the nonlinear effect will be important once it becomes unstable. The transient, however, between stability and instability occurred in a very short time, and the displacement is very small in a stable state.

VII. Results and Discussions

Theoretical flutter boundaries for the test columns without and with an intermediate mass at $\mu_1 = 0.6$ are shown in Fig. 8.

The theoretical boundaries are obtained by taking account of the measured data of the test column. Damping may stabilize or destabilize a nonconservative system. However, the structural damping of the column in the paper is very small. Therefore, Internal damping was neglected in the theoretical flutter predictions. Test results are summarized in Table 4.

The experimental results agreed well with the theoretical flutter or stability predictions on condition that all of the three parameters M_2, J_2, and L_R of the rocket motor are considered.[10] Therefore, it is necessary to consider all of the three parameters of the rocket motor in the analysis of the critical follower force.

The effects of each parameter of the rocket motor on the critical follower thrust are demonstrated in Fig. 9 in case of no intermediate mass. For convenience, the shape of the rocket motor is assumed to be a sphere. In this figure, the solid line with triangle shows the predictions examined by Pflüger's column in which only the mass of the rocket motor is considered. The lowest line with rectangular shape shows the flutter prediction considering the prescribed three parameters. The position and magnitude of the intermediate mass also have a considerable effect on the critical follower force.

VIII. Concluding Remarks

The experimental verification of flutter phenomena of cantilevered columns subjected to an end rocket thrust and having an intermediate mass has been conducted by using a solid rocket motor mounted to the tip end of the columns. The position of the intermediate mass representing the lowest destabilizing effect moves toward the fixed end of the column when the magnitude of the intermediate mass is increased. The highest destabilizing effect occurs at the position of the intermediate mass $\mu_1 = 0.6$. The experimental results agreed well with the theoretical ones if the magnitude of the rocket motor, the rotary inertia of the rocket motor, and the motor distance are all considered. Therefore, consideration of all three parameters M_2, J_2, and L_R of the rocket motor is of vital importance to predict the follower thrust in practice.

References

[1]Beal, T. R., "Dynamic Stability of a Flexible Missile Under the Constant and Pulsating Thrust," *AIAA Journal*, Vol. 3, No. 3, 1965, pp. 486–494.

[2]Wu, J. J., "On the Stability of a Free-Free Beam Under Axial Thrust Subjected to Direction Control," *Journal of Sound and Vibration*, Vol. 43, No. 1, 1975, pp. 45–52.

[3]Beck, M., "Die Knicklast des Einseitig Eingespannten Tangential Gedrückten Stabes," *Zeitschrift für Angewandte Mathematik und Physik*, Vol. 3, No. 3, 1952, pp. 225–228.

[4]Pflüger, A., "Zur Stabilität des Tangential Gedrückten Stabes," *Zeitschrift für Angewandte Mathematik und Mechanik*, Vol. 35, No. 5, 1955, p. 191.

[5]Barsoum, R. S., "Finite Element Method Applied to the Problem of Stability of a Nonconservative System," *International Journal for Numerical Methods in Engineering*, Vol. 3, No. 1, 1971, pp. 63–87.

[6]Kounadis, A. N., and Katsikadelis, J. T., "On the Discontinuity of the Flutter Load for Various Types of Cantilevers," *International Journal of Solids and Structures*, Vol. 16, No. 4, 1980, pp. 375–383.

[7]Park, Y. P., and Mote, C. D., Jr., "The Maximum Controlled Follower Force on a Free-Free Beam Carrying a Concentrated Mass," *Journal of Sound and Vibration*, Vol. 98, No. 2, 1985, pp. 247–256.

[8]Chen, L. W., and Ku, D. M.,"Stability Analysis of a Timoshenko Beam Subjected to Distributed Follower Forces Using Finite Elements," *Computers and Structures*, Vol. 41, No. 4, 1991, pp. 813–819.

[9]Chen, L. W., and Ku, D. M., "Eigenvalue Sensitivity in the Stability Analysis of Beck's Column with a Concentrated Mass at the Free End," *Journal of Sound and Vibration*, Vol. 153, No. 3, 1992, pp. 403–411.

[10]Sugiyama, Y., Katayama, K., and Kinoi, S., "Experiment on Flutter of Cantilevered Columns Subjected to a Rocket Thrust," *Proceedings of the AIAA/ASME/ASCE/AHS/ASC 31st Structures, Structural Dynamics, and Materials Conference* (Long Beach, CA), AIAA, Washington, DC, 1990, pp. 1893–1898.